Journal of Coastal Research	30	1	75–87	Coconut Creek, Florida	January 2014

Hydrochemical Facies and Ionic Ratios of the Coastal Groundwater Aquifer of Saudi Gulf of Aqaba: Implication for Seawater Intrusion

Awni Batayneh[†], Haider Zaman[‡], Taisser Zumlot[†], Habes Ghrefat[†], Saad Mogren[†], Yousef Nazzal[†], Eslam Elawadi[†], Saleh Qaisy[†], Ibrahim Bahkaly[†], and Ahmed Al-Taani[§]

[†]Department of Geology and Geophysics
King Saud University
P.O. Box 2455
Riyadh 11451, Saudi Arabia
awni@ksu.edu.sa

[‡]Department of Geology
Taibah University
P.O. Box 30002
Madinah 41477, Saudi Arabia

[§]UNESCO Chair for Desert Studies and Desertification Control
Yarmouk University
Irbid 21163, Jordan

www.cerf-jcr.org

www.JCRonline.org

ABSTRACT

Batayneh, A.; Zaman, H.; Zumlot, T.; Ghrefat, H.; Mogren, S.; Nazzal, Y.; Elawadi, E.; Qaisy, S.; Bahkaly, I., and Al-Taani, A., 2014. Hydrochemical facies and ionic ratios of the coastal groundwater aquifer of Saudi Gulf of Aqaba: implication for seawater intrusion. *Journal of Coastal Research*, 30(1), 75–87. Coconut Creek (Florida), ISSN 0749-0208.

It is now fairly documented that major ion chemistry of the groundwater can be used to determine an interaction between the groundwater and saline water in the costal aquifers, and that there exists a relationship between total dissolved solids and Cl^-, Na^+, Mg^{2+}, and SO_4^{2-} concentrations of groundwater. This hypothesis is tested on an aquifer located along the Saudi Gulf of Aqaba coast (Red Sea). Groundwater samples collected from 23 locations show the abundance of ions in the order of: $Ca^{2+} > Na^+ > Mg^{2+} > K^+ = Cl^- > SO_4^{2-} > HCO_3^- > NO_3^-$. The Piper trilinear diagram reveals two dominant clusters, *i.e.* the Ca^{2+}–Cl^-–SO_4^{2-} facies and the Na^+–Cl^-–SO_4^{2-} facies. Besides the major chemical compositions, ionic ratios (HCO_3^-/Cl^-, Na^+/Ca^{2+}, Na^+/Cl^-, Ca^{2+}/Cl^-, Mg^{2+}/Cl^-, K^+/Cl^-, SO_4^{2-}/Cl^-, Ca^{2+}/Mg^{2+}, Ca^{2+}/SO_4^{2-}, and Ca^{2+}/HCO_3^-) are used to evaluate the effects of saline water intrusions. Factor analysis of the studied samples demonstrates that changes in the groundwater composition are primarily controlled by mineral dissolution, human activities, weathering of marine sediments, evaporation/salinization of groundwater, and the residence time of water. An attempt has been made to identify hydrochemical processes accompanied with the current intrusion of seawater through the use of ionic exchanges. Following this procedure, about 7.97% mixing rate of seawater intrusion has been estimated for the month of March 2012. Furthermore, the seawater mixing index has also been applied, which resulted in a range of values from 0.395 to 7.922. These results determine 13 of 23 groundwater samples (57%) as saline, with electrical conductivity > 3000 µS/cm.

ADDITIONAL INDEX WORDS: *Groundwater interaction, seawater interaction, hydrochemistry, factor analysis, ionic exchange, SMI, Saudi Arabia.*

INTRODUCTION

Salinization of fresh groundwater aquifers is a common problem in most of the coastal areas around the world (Al-Agha and El-Nakhal, 2004; Barker, Newton, and Bottrell, 1998; Batayneh, 2006; Batayneh, Elawadi, and Al-Arifi, 2010; Mondal *et al.*, 2010; Nwankwoala and Udom, 2011; Silva-Filho *et al.*, 2009). This phenomenon can be attributed to several reasons like gentle coastal hydraulic gradients, low infiltrations, excessive pumping, and local hydrogeological conditions. During the past few decades, researchers produced several publications on the subject from different areas of the world (Diamantis and Petalas, 1989; Kim *et al.*, 2009; Lee and Song, 2007a; Melloul and Collin, 2006; Mondal *et al.*, 2008; Sarma and Krishnaiah, 1976).

DOI: 10.2112/JCOASTRES-D-13-00021.1 received 27 January 2013; accepted in revision 7 April 2013; corrected proofs received 12 May 2013.
Published Pre-print online 5 June 2013.

The study area, located along the eastern cost of Saudi Gulf of Aqaba, is not immune from the effect of seawater intrusion. In addition to the needs of the local population, an increase in the number of tourists (mainly during summer season) has increased a demand for water in the Gulf of Aqaba coast. So far no study has been done to examine hydrochemical behavior of the groundwater in this area; an attempt has been made through this study to evaluate the types of water and their hydrogeochemical characteristics in the target area. The main ionic processes governing the quality and composition of groundwater in the aquifer system of the area is also assessed. Furthermore, the study will help in establishing a basis for an appropriate monitoring system and eventually an improved management of the groundwater resources in the area. To achieve the above objectives, the following tasks are carried out: (1) analysis and interpretation of different data sets to discriminate the effects of different hydrochemical processes; (2) principal component analysis (PCA) for separation of groundwater samples from natural hydrochemical behavior; (3) calculation of ionic deviations to better understand the

hydrochemical processes; and (4) development of an index, called seawater mixing index (SMI), for evaluating a relative degree of seawater mixing.

MATERIALS AND METHODS

Description of the Study Area

The NNW-SSE-oriented Red Sea zone (Figure 1), which is located between 12° N and 28° N, is about 1930 km long and 270 km wide (Fahmy, 2003; Maillard and Soliman, 1986). In the north, the sea splits into the western shallow Gulf of Suez and the eastern deep Gulf of Aqaba. The Gulf of Aqaba (Figure 1) is located in the subtropical arid climate zone between 28–29°30′ N and 34°30′–35° E. It is about 180 km long and has a maximum width of 25 km. The maximum depth in the Gulf of Aqaba is about 1830 m, with a mean depth of about 800 m (Morcos, 1970). The Gulf of Aqaba is semienclosed and is connected to the Red Sea by the Strait of Tiran, which has a sill depth of about 260 m (Hall, 1975). The marine environment in the Gulf area is surrounded by arid continental environments (the African-Arabian deserts) that cause an extremely high temperature and low precipitation. These conditions have led to the evolution of unique, and hence internationally important, coral reef and marine ecosystems in the area, which are particularly susceptible to damage from pollution or other forms of environmental degradation (Assaf and Kessler, 1976). The Gulf of Aqaba also provides an important source of economic activities in terms of sea transportation, tourism development, and other industrial activities along the coastal areas.

Geological and Hydrogeological Characteristics

A regional-scale geological map (1:250,000 scale) for northwestern Saudi Arabia has been prepared by Clark (1986). Some other geological studies have been reported by Wyn Hughes *et al.* (1999) and Wyn Hughes and Johnson (2005). According to these studies, the Oligocene Sharik Formation, which consists of conglomerate and sandstone, is determined as the oldest sedimentary rock unit, which unconformably overlies the Proterozoic basement (Figure 1). The metamorphic basement varies in composition from monzogranite to alkali feldspar granite. The Sharik Formation is then unconformably overlain by deep marine Early Miocene Musayr Formation, which consists of sandstone, conglomerate, limestone, shale, and gypsum (undifferentiated), which in turn is overlain by marine mudstones, carbonates, and evaporites (undifferentiated) of the Middle Miocene age of Nutaysh Formation. The Middle Miocene marine sediments are then unconformably overlain by the Late Miocene Bad' Formation of gypsum and anhydrite. The Bad' Formation is then unconformably overlain by sandstone, conglomerate, sand, and local gypsum of Lisan Formation of Pleistocene age. The youngest unconsolidated Quaternary deposits at the surface consist of sands and gravels.

The area under study is located in an extremely arid zone with annual average precipitation of 20 mm. Rainfall generally occurs during the winter months; however, some of the years pass without any rainfall at all, whereas others receive heavy rainfall of short duration, causing ephemeral flooding. The climate of the region is very hot in summer, with temperatures in excess of 47°C (Al-Ahmadi, 2009). The primary sources of water in Saudi Arabia are aquifers and basins that receive feeding/recharging from annual rainfall. Two types of groundwater aquifers have been identified: the shallow alluvial aquifers beneath the wadi systems, and deep rock aquifers, usually hosted by sandstone and limestone (Batayneh *et al.*, 2012a). The coastal plain of the Saudi Gulf of Aqaba is approximately 0.5 to 20 km wide and is accessible by one modern highway joining Saudi Arabia in the south with Jordan to the north. The alluvial shallow aquifer is the primary source of water for agriculture, domestic, and industrial uses in the region. The recharge to this aquifer takes place either from the elevated areas in the east, or due to local surface-water infiltrations. Water levels vary from about 60 m above sea level in the headwaters to about 10 m in the coastal plain.

Groundwater Sampling

Twenty-three groundwater samples were collected during March 2012 from shallow alluvial bored production wells having depths ranging from 10 m at the coastal area to 80 m inland distributed throughout the area. Methods adopted for the collection and analysis of water samples are essentially the same as suggested in the standard procedure of the American Public Health Association (APHA, 1998). Samples were collected in the acid-cleaned 1000-mL-capacity polyethylene bottles. The hydrogen ion concentration (pH) and electrical conductivity (EC) were measured in the field using portable pH and EC meters (Hanna Instruments, Ann Arbor, Michigan, U.S.A.). Total dissolved solids (TDS) were measured using a conductivity probe that detects the presence of ions in water. The TDS analyses were performed using Orion 5 Star Conductivity Meter (Thermo Scientific, Beverly, Massachusetts, U.S.A.). The sodium, potassium, magnesium, and calcium ions were determined by atomic absorption spectrophotometry. Bicarbonate and chloride were analyzed by volumetric methods. Sulfate was estimated by the colorimetric and turbidimetric methods. Silicon dioxide was colorimetrically analyzed by ammonium molybdate method and alkalinity was determined by titration method. Nitrate was measured by ionic chromatography. Analytical precision for the measurements of cations and anions, obtained from ionic balance error (IBE), was computed in terms of ions expressed in meq/L. The value of IBE is observed to be within a limit of ±5% (Domenico and Schwartz, 1990). Precise locations of the sampling points (as shown in Figure 1) were determined in the field using a Garmin instrument (Garmin Ltd., Southampton, U.K.).

Statistical Analysis

Parametric statistical methods are used to calculate normal statistical values including range, arithmetic mean, and standard deviation for groundwater quality parameters such as pH, EC, TDS, Na^+, K^+, Ca^{2+}, Mg^{2+}, Cl^-, HCO_3^-, SO_4^{2-}, NO_3^-, and SiO_2. PCA is another popular statistical multivariate technique, by which the most important components contributing to the data structure and their interrelationships can be identified. It is a simple mathematical procedure used for data reduction without any elaborate assumptions (Sharma, 1996), which enables one to describe the information with considerably fewer variables than those originally present. For the Saudi Gulf of Aqaba, hydrochemical data are

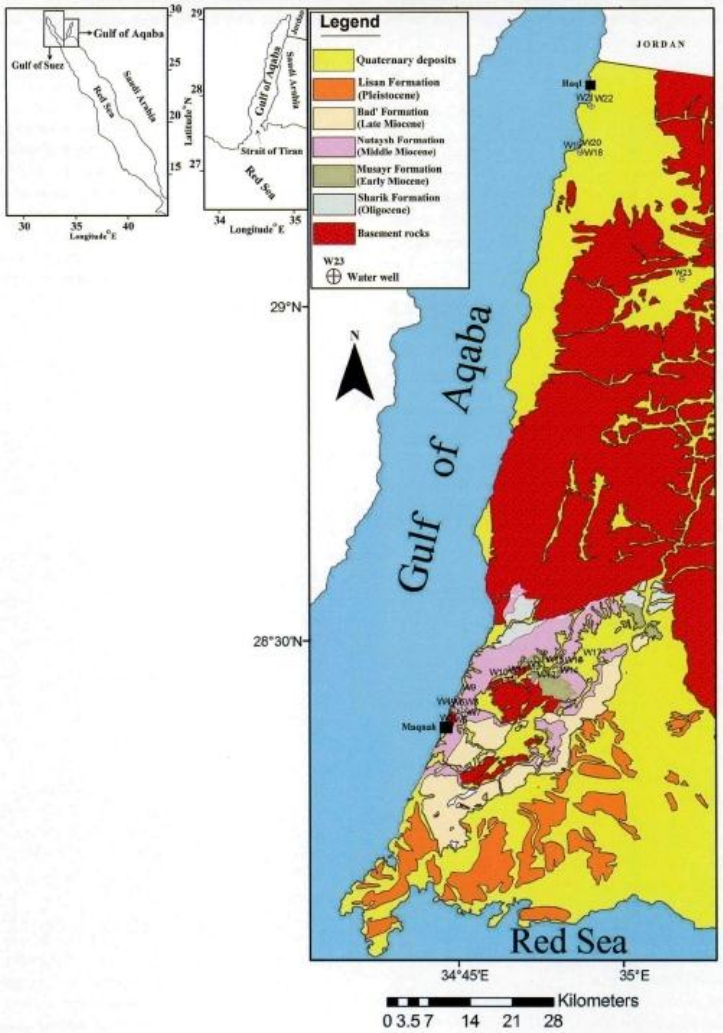

Figure 1. Geological map for the Gulf of Aqaba–Red Sea region (modified after Clark, 1986). Black circles indicate borehole locations. Inset maps show the Red Sea, the Gulf of Suez, the Gulf of Aqaba, and the Straits of Tiran.

analyzed with PCA using SPSS software package to quantify the effects of natural chemical weathering and seawater intrusion on the chemical composition of groundwater in the coastal setting.

Ionic Exchanges

Ionic deviations are calculated to better understand the occurrences of hydrogeochemical processes in the coastal aquifers. Calculation of ionic deviations (Δ) is made by

comparing the measured concentration of each constituent with its theoretical concentration of a known freshwater–seawater mixture estimated from the Cl^- concentration in the sample (Mondal *et al.*, 2011) as:

$$\Delta C_i = C_{i,\text{sample}} - C_{i,\text{mixed}} \quad (1)$$

where ΔC_i is the ionic deviation of ion i; $C_{i,\text{sample}}$ is the measured concentration of ion (i) in the sample, and $C_{i,\text{mixed}}$ is the theoretical concentration of ion (i) for the freshwater–seawater mixture. The theoretical mixture concentrations are calculated by taking into account seawater contribution (f_{sea}), which is based on chloride contents in the sample ($C_{\text{Cl, sample}}$), the freshwater Cl^- concentration ($C_{\text{Cl,f}}$), and the seawater Cl^- concentration ($C_{\text{Cl,sea}}$):

$$f_{\text{sea}} = \frac{(C_{\text{Cl,sample}} - C_{\text{Cl,f}})}{(C_{\text{Cl,sea}} - C_{\text{Cl,f}})} \quad (2)$$

This allows calculation of seawater contents (%) in each sample of the study area. The seawater contribution is then used to calculate theoretical concentration of each ion:

$$C_{i,\text{mixed}} = f_{\text{sea}} \times C_{i,\text{sea}} + (1 - f_{\text{sea}}) \times C_{i,\text{f}} \quad (3)$$

In these calculations the Cl^- is taken as a conservative tracer (Mondal *et al.*, 2011), which in fact usually cannot be removed from the aquifer system because of its high solubility. The only inputs of Cl^- are either from the aquifer matrix salts or from salinization sources like seawater intrusion.

Seawater Mixing Index

For quantitative estimation of the relative degree of seawater mixing in the sampled water, the SMI parameter is adopted. This parameter is based on the concentration of four major ionic constituents in seawater (*i.e.* Na^+, Mg^{2+}, Cl^-, and SO_4^{2-}) due to their abundance, as expressed by the following formula:

$$\text{SMI} = a \times \frac{C_{\text{Na}}}{T_{\text{Na}}} + b \times \frac{C_{\text{Mg}}}{T_{\text{Mg}}} + c \times \frac{C_{\text{Cl}}}{T_{\text{Cl}}} + d \times \frac{C_{\text{SO}_4}}{T_{\text{SO}_4}} \quad (4)$$

where constants a, b, c, and d denote a relative proportion of Na^+, Mg^{2+}, Cl^-, and SO_4^{2-} ($a = 0.31$, $b = 0.04$, $c = 0.57$, and $d = 0.08$) in seawater, respectively; C is the calculated concentration of groundwater samples in mg/L; and T is the calculated regional threshold values of the selected ions in groundwater samples, which can be estimated from the interpretation of cumulative probability curves.

RESULTS AND DISCUSSION

Groundwater Chemistry

Table 1 gives the general outline of the statistical results for the groundwater samples ($N = 23$). The pH values are slightly alkaline and do not show any significant difference, and are comparable with drainage water that passes through the marine sedimentary lithology. The pH values of rainwater (average of 5.1, WHO, 1984) are low when compared with the values of groundwater samples (ranging from 7.02 to 7.82, Table 1). The EC values for the studied samples are in a range between 830 and 20,450 μS/cm (Table 1). Examining EC, Mondal *et al.* (2008) classified the groundwater into (1) fresh (<1500 μS/cm), (2) brackish (1500–3000 μS/cm), and (3) saline (>3000 μS/cm). On the basis of this classification, about 57% of the groundwater samples are categorized as saline, 39% brackish, and only 4% fresh in quality.

Elevated levels of TDS in groundwater samples were observed where the vast majority of wells showed values above 800 and up to 10,018 mg/L (Table 1). Only one borehole (23) exhibits acceptable TDS value for drinking water (406 mg/L). Although drinking water containing more than 500 mg/L is undesirable (WHO, 2008), such water is commonly used in this region as less mineralized water is rare or not available. However, groundwater with salinity greater than 3000 mg/L is generally suitable for stock (sheep are common is the area). The TDS values are likely elevated due to dissolution of aquifer materials, leaching soluble salts after irregular rainfall events. In addition, high TDS levels may be due to sea spray, intermittent tidal influences, and seawater intrusion. The spatial distribution of TDS in groundwater illustrates that high occurrences of TDS are located farther coastward (except for wells 14 and 15). This indicates that dissolved salts are primarily related to saltwater intrusion in the vicinity of the shoreline caused by intensive pumping of groundwater and enhanced probably by evaporative concentration. Besides, dissolving salts from evaporate formation and carbonate layers are contributing factors to high TDS. Additionally, in winter seasons, storms batter the coast and water near the shore becomes rough and encroaches toward land. During summer seasons, when the demand for water increases and over-abstraction of groundwater becomes widespread, the saline water finds its way through tidal channels and it admixes with shallow coast aquifers. Excessive withdrawal of groundwater coupled by high evaporation and significant decrease in recharge particularly during drought years contributes substantially to increased groundwater contamination by seawater. As for the other wells (14, 15) with relatively higher salinity eastward, this is likely related to leaching of nearest localized evaporate outcrops and agricultural discharges after excessive irrigation and overextraction of groundwater.

TDS data of the upper northern wells (except well 23) exhibited significantly higher TDS values compared with those located in the lower south of the study area. In addition to seawater intrusion, surface drainage pattern in the uppermost northern part is directed to the west and northwest, where wells 18–22 are located down-gradient of water drainage. After intense rainfall, salts and dissolved minerals from the surrounding geologic formations are transported down-gradient following the general flow direction to end up in groundwater. These wells also lie within the beach area and are subjected to regular seawater seepage, particularly during spring tides. We have also observed during groundwater sampling that these wells are extensively abstracted for public use, livestock farming, and irrigation as they are located in proximity to human settlements. Additionally, groundwater wells may have also been enriched in mineral content by irrigation, where inhabitants rely also on agricultural activities for their livelihoods.

On the other hand, surface water runoff is not directed to those wells located in the lower south area and the rate of groundwater extraction is relatively low compared with the northern wells, which is consistent with the lower TDS value

Table 1. *Hydrochemical results for 23 studied wells.TDS = total dissolved solids, EC = electrical conductivity, Min = minimum, Max = maximum, SD = standard deviation.*

Borehole no.	pH	TDS (mg/L)	EC (μS/cm)	Concentration (meq/L)								
				Na^+	Ca^{2+}	K^+	Mg^{2+}	HCO_3^-	SO_4^{2-}	Cl^-	NO_3^-	SiO_2
1	7.52	1780	3620	14.7	13.4	0.49	6.14	3.70	6.29	24.03	0.68	0.87
2	7.42	1456	2980	11.2	12.9	0.50	5.55	3.00	6.50	20.03	0.66	0.78
3	7.43	1471	3020	10.4	23.7	0.89	5.43	3.10	16.59	20.03	0.65	0.72
4	7.52	1578	3240	9.8	18.6	0.44	4.94	3.61	8.60	21.01	0.63	0.70
5	7.67	1411	2880	8.3	14.5	0.18	4.77	3.51	3.71	20.03	0.65	0.60
6	7.82	1400	2857	14.7	23.2	0.07	4.80	2.61	19.47	20.03	0.65	0.93
7	7.55	1683	3440	11.8	18.4	0.42	6.79	2.10	12.62	22.03	0.68	0.93
8	7.32	1184	2415	5.7	16.5	0.25	3.46	2.10	7.10	16.02	0.68	0.80
9	7.45	1784	3640	15.3	15.5	1.00	6.03	2.51	13.20	22.03	0.11	0.45
10	7.36	1319	2686	19.5	15.8	0.21	4.87	2.20	19.26	18.02	0.73	0.37
11	7.59	985	2010	4.9	11.7	0.27	2.90	2.70	2.50	14.02	0.65	0.48
12	7.6	1048	2140	4.7	10.7	0.12	3.06	2.29	3.71	12.02	0.61	1.02
13	7.54	1878	3830	11.6	19.9	0.15	5.94	2.70	4.21	30.04	0.69	0.78
14	7.42	3028	6180	20.9	21.3	0.26	11.00	2.61	6.20	44.06	0.77	0.45
15	7.4	2583	5270	17.4	22.8	1.01	7.92	3.00	7.29	38.05	0.74	0.85
16	7.8	1124	2295	4.7	13.1	0.10	3.13	2.51	1.92	16.02	0.63	0.37
17	7.75	800	1632	2.8	12.3	0.40	2.17	2.80	2.50	12.02	0.45	0.28
18	7.18	3080	6250	79.0	25.3	0.60	2.23	1.80	8.50	96.13	0.76	0.72
19	7.05	6703	13,680	115.8	23.0	0.61	2.39	2.10	6.89	132.2	0.74	0.65
20	7.02	10018	20,450	168.8	44.9	0.73	4.58	1.90	6.29	210.3	0.69	0.77
21	7.04	2142	4370	54.4	14.5	0.51	1.72	2.51	29.19	38.05	0.73	0.65
22	7.08	5010	10,220	71.3	33.8	0.54	2.38	1.80	9.68	96.13	0.44	0.57
23	7.62	406	830.0	9.0	11.9	0.13	0.97	2.61	12.74	6.01	0.71	0.50
Min	7.02	406	830.0	2.8	10.7	0.07	0.97	1.8	1.92	6.00	0.11	0.28
Max	7.82	10,118	20,450	168.7	44.9	1.0	11.0	3.7	29.19	210.3	0.77	1.02
Mean	7.44	2342.2	4779.8	29.9	19.0	4.49	4.49	2.6	9.34	41.23	0.64	0.66
SD	0.24	2183.0	4454.6	41.7	8.0	0.28	2.29	0.54	6.66	48.51	0.14	0.20

observed for the southern wells. However, well 23 exhibited the least TDS level, where it has been probably enriched in mineral content by dissolution of naturally occurring soluble minerals of underground formations, rather than the effects of seawater intrusion. In addition, saline groundwater might occur in well 23 due to both high evaporation and dissolution of evaporate minerals.

Assessment of TDS distribution pattern in groundwater aids public water supplies and regulatory agencies in targeting zones of lower groundwater TDS concentration by relocating wells or by mixing multiple groundwater sources. The artificial recharging of aquifers with fresh groundwater or harvested rainwater can reduce groundwater salinization as the recharge increases the groundwater pressure and reverses the pressure gradient caused by coastal groundwater abstraction. TDS trends also help in quantifying the optimum groundwater abstraction rate without major increase in salinity for sustainable utilization of this water source. Additionally, saltwater intrusion into the shallow groundwater aquifers, particularly those in proximity to the coast, can be minimized by construction of tidal and subsurface barriers.

The obtained results also show that Ca^{2+} and Na^+ are the dominant cations in the studied samples, whereas Cl^- and SO_4^{2-} are the dominant anions. The range of Ca^{2+} concentration is 10.70–44.92 meq/L and that of Na^+ is 2.78–168.73 meq/L (Table 1). In addition to its relatively high mobility in water, high Ca^{2+} percentages (46% of the total cation) are mainly due to leaching from minerals, and rocks weathering (gypsum and anhydrite). The presence of Na^+ as a second highest concentration (41%) could be attributed to rocks weathering (halite marine sediment), sea-salt deposition, and marine intrusion. The concentration of Mg^{2+} is 12% of the total cations, whereas K^+ is observed as the lowest concentrated element in the studied samples (Table 1), which is probably due to its low mobility in water.

The presence of Cl^-, SO_4^{2-}, HCO_3^-, and NO_3^- in respective order have been observed as dominant anions (Table 1). The range of concentrations for Cl^- and SO_4^{2-} are 6.00–210.28 meq/L and 1.92–29.19 meq/L, respectively (Table 1).The high Cl^- percentage (69% of the total anions) can either be attributed to weathering of halite or to Na^+-related sources (including sea-salt sprays). The SO_4^{2-} concentration accounts for 23% of the total anions in the studied groundwater, which could mainly be attributed to weathering processes of the marine-origin gypsum and anhydrite. Next of order is HCO_3^- (alkalinity), which with average concentration of 2.6 meq/L represents about 8% of the total anion concentration. HCO_3^- in the samples likely originated from granitic rocks weathering and decay of organic matter in the soil. Following the Spearmen's correlation matrix (Table 2) highly positive correlations are observed between Na^+ and Cl^- ($r = 0.98$), Na^+ and Ca^{2+} ($r = 0.80$), and Ca^{2+} and Cl^- ($r = 0.86$), as well as between pH and HCO_3^- ($r = 0.50$), clearly corroborating this interpretation. On the other hand, the pH values show highly negative correlations (*i.e.* $r = -0.72$, -0.72, -0.78, and -0.72) with EC, TDS, Na^+, and Cl^-, respectively. Good correlations between TDS, EC, Na^+, Ca^{2+}, Cl^-, and other anions suggest that groundwater resources in the study area are affected by salinity enrichment in terms of major ions except SiO_2 and NO_3^- (Table 2).

Table 2. *Cross-correlation among major chemical constituents in the shallow groundwater. Large correlation values (>0.50) are marked in bold. EC = electrical conductivity, TDS = total dissolved solids.*

	pH	EC	TDS	SiO_2	Na^+	Ca^{2+}	K^+	Mg^{2+}	HCO_3^-	Cl^-	SO_4^{2-}	NO_3^-
pH	1											
EC	**−0.72**	1										
TDS	**−0.72**	**0.99**	1									
SiO_2	−0.08	0.10	0.10	1								
Na^+	**−0.78**	**0.95**	**0.95**	0.07	1							
Ca^{2+}	−0.60	**0.86**	**0.86**	0.19	**0.80**	1						
K^+	−0.52	0.41	0.41	0.07	0.37	0.42	1					
Mg^{2+}	0.12	0.00	0.00	0.18	−0.21	0.11	0.20	1				
HCO_3^-	**0.50**	−0.45	−0.45	0.04	−0.53	−0.43	0.00	0.32	1			
Cl^-	**−0.72**	**0.98**	**0.98**	0.09	**0.98**	**0.86**	0.39	−0.10	−0.51	1		
SO_4^{2-}	−0.29	−0.08	−0.08	0.06	0.06	0.05	0.15	−0.09	−0.13	−0.08	1	
NO_3^-	−0.16	0.11	0.11	0.31	0.16	0.08	−0.31	0.09	0.01	0.15	0.03	1

Geochemical Classification

Ionic concentrations have been plotted on a Piper trilinear diagram (Piper, 1944) to better understand the hydrochemical processes operating in the groundwater system of the area. This diagram (Figure 2) for the study area shows two types of water with variable concentrations of major ions. Major clusters are observed for Ca^{2+}–Cl^-–SO_4^{2-} and Na^+–Cl^-–SO_4^{2-} facies, indicating that groundwater in the area is mainly made of mixtures of earth alkaline and alkaline metals and predominantly Cl^-–SO_4^{2-} water. Cl^- is found as the dominant anion followed by SO_4^{2-}. Due to the influence of recharge on the aquifer systems in the area, a relatively higher SO_4^{2-}/Cl^- (in meq/L) ratio is obtained compared with the effects from seawater. This reveals that only a part of the sulphate contents could have drawn from seawater and a significant proportion came from other saline sources that differentially enriched the groundwater in the study area. This sulphate enrichment is accompanied by increases in calcium and magnesium, suggesting a nonmarine origin for these ions. Because of the coastal aquifer vulnerability to marine intrusion, the ion exchange processes assume great significance in the salinized zones, and is considered an important factor regulating ion concentrations in the groundwater (Appelo and Postma, 2005). The classic bibliography on ion exchange processes in the coastal aquifers is presented by Howard and Lloyd (1983) and Tellam and Lloyd (1986). According to them, the appearance of Ca^{2+}–Cl^- facies in the coastal aquifer reflects the role of inverse ion exchange, whereas the presence of Na^+–HCO_3^- facies indicate activities of direct exchange. The predominance of Ca^{2+}–Cl^- facies in much of the studied aquifer clearly indicates the existence of inverse ion exchange. As a matter of observations, the groundwater generally tends to acquire chemical compositions similar to that of seawater (that is more dissolved and has a relative increase in chloride ion) the longer they remain underground and farther they travel.

Deterioration of groundwater quality in the wells located near the coast is observed that is most likely caused by increasing anthropogenic activities. Another probable reason behind this deterioration is the length of groundwater flow paths, which are characterized by various dyke intrusions and fractured zones (Lee and Song, 2007b; Silva-Filho *et al.*, 2009). On the basis of the results of Piper classification (Figure 2), the sedimentary layers in the study area are classified as marine in origin, in which the appearance of $Ca^{2+}+Na^+$–$Cl^-+SO_4^{2-}$ facies is characterized by low concentrations of HCO_3^- and relatively high concentrations of Ca^{2+}, Na^+, Cl^-, and SO_4^{2-}. These high-concentration elements are mainly distributed in the recent coastal marine sediments, but their association with deep ancient marine waters could also yield $Ca^{2+}+Na^+$–$Cl^-+SO_4^{2-}$ facies.

Lineament studies of the southern Jordan are mapped using gravity data and field studies (Batayneh, Ghrefat, and Diabat, 2012b) and lineament study of the northwestern Saudi area from aeromagnetic data (Elawadi *et al.*, 2013) were mapped to understand the tectonic origin of these lineaments in relation to the Dead Sea Transform Fault (DSTF) and the Red Sea opening. Lineament also provides important information on subsurface fractures that may control the movement and storage of groundwater. Subsurface permeability is a function of fracture density of rocks (Sharma, 1997). Four sets of lineaments trending E-W, NW-SE, NE-SW, and N-S are identified. Potential data and field studies indicate that most of the lineaments are extensional features that correspond to normal faults. Most of these were subsequently reactivated into strike–slip shear fractures. The concentrations of lineaments are more in areas adjacent to the DSTF zone area in the western side than the eastern region. Therefore, the density of lineaments increases toward the Gulf of Aqaba-DSTF area.

Ionic Ratios/Relations and Sources of Major Components

Ionic ratios of water have been often used to evaluate salinity and origin of the groundwater in coastal areas (Barbecot *et al.*, 2000; El Moujabber *et al.*, 2006; Kim, Kim, and Chang, 2003; Sanchez-Martos *et al.*, 2002). The ionic relationships that are commonly used includes: HCO_3^-/Cl^-, Na^+/Ca^{2+}, Na^+/Cl^-, Ca^{2+}/Cl^-, Mg^{2+}/Cl^-, K^+/Cl^-, SO_4^{2-}/Cl^-, Ca^{2+}/Mg^{2+}, Ca^{2+}/SO_4^{2-}, and Ca^{2+}/HCO_4^{2-} (Table 3). The HCO_3^-/Cl^- ratio for freshwater recharge is higher than the seawater ratio (0.0069). However, it registered a gradual increase and became close to the seawater ratio as TDS increased (Figure 3a), indicating an increase in seawater intrusion. As shown in Table 2, TDS is a perfect surrogate for Cl^- ($r=0.98$), which can consequently present the HCO_3^-/Cl^- ratio as a good indicator for salinization due to seawater encroachment. The Na^+/Ca^{2+} ratio, which is indicative of cation exchange reaction (Edet and Okereke, 2002),

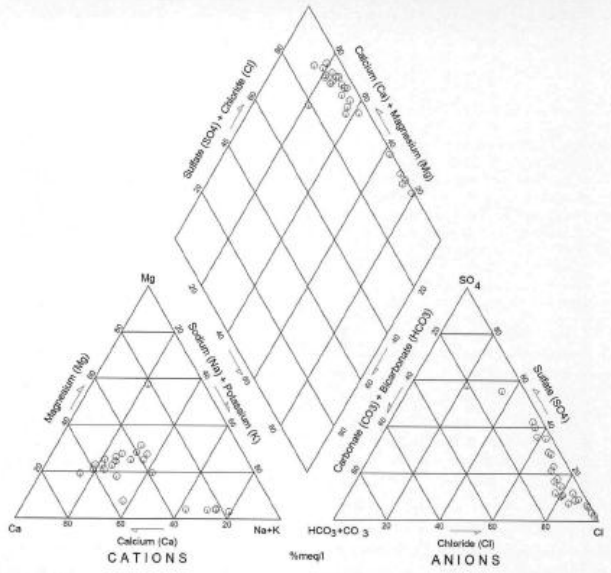

Figure 2. Piper diagram for the studied groundwater samples.

generally reveals a mixed behavior, but a visible enhancement is observed upon increase in TDS (Figure 3b).

As shown in Figure 3c and Table 3, the ratios of Na^+/Cl^- show no significant correlation with the TDS level ($R^2 = 0.005$) but give almost similar values to that of seawater (coefficient of variation [CV] = 0.52). This is because they accompanied each other when seawater intrusion occurred. Thus, this ratio may not be a good indicator for the salinization process. The ratios of Ca^{2+}/Cl^- (Figure 3d) generally exhibit a good negative correlation with TDS ($R^2 = 0.73$). These ratios decrease as TDS increases, which is most likely caused by Cl^- enrichment in the groundwater due to saline water intrusion. As shown in Figures 3e and 3f, the ratios of Mg^{2+}/Cl^- and SO_4^{2-}/Cl^- differ moderately from each other (*i.e.* CV = 0.497 and 1.080, respectively) and indicate a moderate negative correlation with TDS ($R^2 = 0.36$ and 0.33, respectively). The ratio of K^+/Cl^+ shows weak correlation with TDS, *i.e.* $R^2 = 0.15$ (Figure 3g). For a given range of TDS this ratio shows great variations, so could not be taken as a good criterion for evaluating seawater intrusion. The ratios of Ca^{2+}/Mg^{2+} and Ca^{2+}/SO_4^{2-} are not closely correlated with TDS values ($R^2 = 0.11$ and 0.10, respectively), and show no variation in spite of increase in TDS values (Figures 3h and 3i). The ratio of Ca^{2+}/HCO_3^- in turn shows good positive correlation with TDS ($R^2 = 0.69$, Figure 3j), where its low value corresponds to low TDS and vice versa. On the basis of these explanations, it can be concluded that some of the ionic ratios can provide useful information to delineate the extent of groundwater salinization, although they may have been affected by certain artifacts in the course of groundwater samplings and the subsequent chemical analyses.

Statistical Approach to Groundwater Chemistry

With increasing number of chemical and physical variables in groundwater, a wide range of multivariate statistical techniques are now in use. PCA is frequently applied as a quantitative approach for plotting and interpreting the data concerning the groundwater pollutants and geochemistry. Batayneh and Zumlot (2012), Cloutier *et al.* (2008), Farnham *et al.* (2003), Farooq *et al.* (2010), Liu, Lin, and Kuo (2003), and Love *et al.* (2004) adopted the PCA technique to determine groundwater contamination, geochemical evolution, and rock–water interactions. In addition, multivariate analyses have been used to interpret a relationship among the chemical variables, the processes involved, and the regional impact of human activities on groundwater composition (Briz-kishore and Murali, 1992; Razack and Dazy, 1990; Subyani and Al-Ahmadi, 2010). Moreover, multivariate statistical methods can also help in understanding groundwater flow in complex aquifer systems (Farnham *et al.*, 2000; Stetzenbach *et al.*, 2001).

Since the frequency diagrams of chemical parameters do not follow a normal distribution; the PCA has been carried out for logarithmic transformation of the data set due to its closeness to normality condition required for these analyses. Standard-

Table 3. *Ionic ratios for 23 groundwater samples from the study area. SD = standard deviation, CV = coefficient of variation, GOA = Gulf of Aqaba.*

Well No.	HCO_3^-/Cl^-	Na^+/Ca^{2+}	Na^+/Cl^-	Ca^{2+}/Cl^-	Mg^{2+}/Cl^-	SO_4^{2-}/Cl^-	K^+/Cl^-	Ca^{2+}/Mg^{2+}	Ca^{2+}/SO_4^{2-}	Ca^{2+}/HCO_3^-
1	0.265	1.259	0.397	0.315	0.088	0.354	0.022	3.601	0.889	1.189
2	0.258	0.990	0.362	0.365	0.095	0.439	0.028	3.843	0.831	1.417
3	0.266	0.501	0.335	0.670	0.093	1.123	0.049	7.204	0.597	2.516
4	0.295	0.606	0.304	0.501	0.081	0.554	0.023	6.225	0.904	1.698
5	0.301	0.655	0.269	0.410	0.082	0.251	0.010	5.019	1.635	1.360
6	0.224	0.728	0.476	0.654	0.082	1.32	0.004	7.966	0.497	2.921
7	0.164	0.737	0.348	0.472	0.106	0.776	0.021	4.469	0.608	2.880
8	0.225	0.400	0.232	0.581	0.074	0.600	0.017	7.841	0.968	2.579
9	0.196	1.130	0.450	0.398	0.094	0.812	0.050	4.244	0.491	2.033
10	0.210	1.414	0.700	0.495	0.093	1.448	0.013	5.345	0.342	2.361
11	0.332	0.480	0.226	0.470	0.071	0.241	0.021	6.623	1.948	1.417
12	0.329	0.508	0.256	0.503	0.087	0.418	0.011	5.763	1.204	1.531
13	0.155	0.671	0.251	0.374	0.068	0.190	0.006	5.521	1.973	2.416
14	0.102	1.127	0.308	0.273	0.085	0.191	0.007	3.204	1.434	2.688
15	0.136	0.878	0.297	0.338	0.071	0.259	0.029	4.734	1.303	2.491
16	0.270	0.415	0.192	0.462	0.067	0.162	0.007	6.903	2.851	1.714
17	0.401	0.260	0.150	0.577	0.062	0.282	0.037	9.318	2.050	1.439
18	0.032	3.589	0.533	0.148	0.008	0.120	0.007	18.672	1.240	4.600
19	0.027	5.768	0.568	0.098	0.006	0.071	0.005	15.907	1.394	3.604
20	0.016	4.310	0.520	0.121	0.007	0.041	0.004	16.189	2.980	7.759
21	0.113	4.314	0.927	0.215	0.015	1.039	0.015	13.876	0.207	1.895
22	0.032	2.422	0.481	0.199	0.008	0.136	0.006	23.408	1.455	6.150
23	0.746	0.865	0.972	1.123	0.055	2.873	0.024	20.280	0.391	1.505
Mean	0.222	1.479	0.415	0.425	0.065	0.596	0.018	8.963	1.226	2.616
SD	0.157	1.522	0.216	0.223	0.032	0.643	0.014	5.945	0.756	1.609
CV	0.710	1.029	0.520	0.524	0.497	1.080	0.754	0.663	0.617	0.615
GOA water	0.0069	19.1662	0.556	0.0265	0.0726	0.1810	0.0228	0.319	0.152	3.8290

ization has been applied to the log-normal distribution to ensure that each variable is weighted equally. Log transformation of positively skewed chemical parameters as well as data standardization are commonly carried out by multivariate statistical analysis (Cloutier *et al.*, 2008). Results obtained after the PCA show five PCs (Table 4), which account for 93.77% of the total variance.

Factor 1, which is 42.71% of the total data variance, presents significantly high positive loading for EC, Ca^{2+}, Na^+, and Cl^-, and negative loading for pH (Table 4). These high-loading elements are interpreted as being related to salinity in the form of NaCl. The high Na^+ and Cl^- contents detected in certain samples may suggest the dissolution of chloride salts. Dissolution of halite in water releases equal concentrations of Na^+ and Cl^- into the solution. Enrichment of Na^+ and Cl^- is also possible, which may be related to urban wastewaters and high rate of evapotranspiration. Negative association of this factor with pH may suggest a mixed zone of water formed during their contacts with diabase dykes, which promotes pyrite oxidation, increasing SO_4^{2-} concentration and decreasing pH level.

Factor 2 accounts for 18.26% of the total variance and contains a high positive loading for K^+ and SO_4^{2-} (Table 4). This behaviour is probably due to a contribution from agricultural activities and weathering of K^+ feldspar from the surrounding basement rocks (mainly granite). High loadings for SO_4^{2-} could also be caused by marine processes (marine intrusion or marine sedimentation).

Factor 3, which corresponds to 12.81% of the total data variance, represents a significant positive loading for Mg^{2+} (Table 4) and is related to evaporation/salinization of the groundwater.

Factor 4 is attributed to SiO_2 (Table 4), which is a major constituent resulting from the hydrolysis of K-feldspars (weathering process) and plagioclase. This factor is responsible for 10.59% of the variance in the data set, and is probably related to the contact time along the flow path (principal fractures), which is long enough for significant dissolution of silicate minerals. A representative example of this process can be observed in well 6, where relatively higher concentration of SiO_2 and pH have been found (Table 1), indicating a long path in contact with granite/gneiss. Despite the elevated SiO_2 concentration in wells 1, 7, 8, 12, and 15 (Table 1), the pH values show no increase, which is probably due to its lower water residence time.

Factor 5 is primarily related to HCO_3^- (Table 4), which is the major constituent resulting from evaporation/salinization of groundwater or dissolution of marine sediments. This factor is responsible for 9.40% of the total data set.

Seawater Mixing

On the basis of Equations (1), (2), and (3), a mixing composition of seawater and freshwater is calculated and then compared with the measured concentrations in the studied groundwater samples. The resulting ionic exchanges in all the studied wells are presented in Table 5. The mixing rate in all wells (W-1–W-23) during the sampling period was about 7.97%.

Figure 4 shows ionic exchanges (ΔC) calculated for Ca^{2+}, Na^+, Mg^{2+}, K^+, Cl^-, SO_4^{2-}, and HCO_3^- in all studied wells during March 2012. The most marked pattern is observed for Na^+ and Ca^{2+}. The heterogeneous patterns shown by these two ions are most probably due to a direct contact between Na^+-enriched water (seawater) with Ca^{2+}-enriched water (fresh groundwater). The ionic exchange for Na^+ is usually positive since fresh

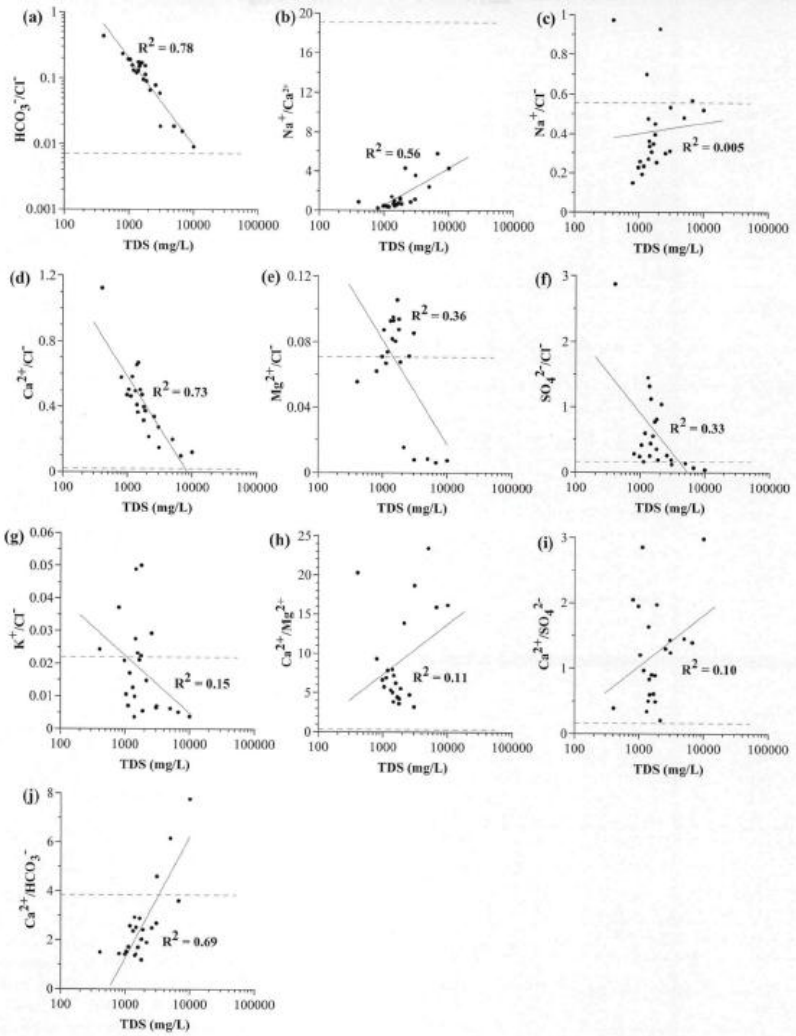

Figure 3. Ionic ratios of the studied groundwater with respect to total dissolved solids levels. Dashed line indicates a ratio for the Gulf of Aqaba.

groundwater contains only a small amount of Na^+. However, all the studied wells revealed negative values except for well W-23 during the study period (see Figure 4). The negative value of ΔC_{Na} indicated a simple mixing between the groundwater and seawater, as indicated by the high EC values.

A higher value for Na^+ in the studied groundwater is probably attributed to direct cation exchange process at the seawater–freshwater interface. Usually and as a result of carbonate dissolution, the composition of fresh groundwater in coastal areas is often dominated by Ca^{2+} and HCO_3^-

Table 4. *Principal component loadings and the estimated variances for five components obtained through Varimax normalized rotation. EC = electrical conductivity.*

Parameters	Factor 1	Factor 2	Factor 3	Factor 4	Factor 5
pH	−0.86	−0.18	0.31	−0.09	0.08
EC (μS/cm)	**0.96**	−0.01	0.22	0.07	−0.12
Ca^{2+} (mg/L)	**0.78**	0.17	0.29	0.12	−0.30
K^{+} (mg/L)	0.12	**0.89**	0.26	−0.15	−0.10
Mg^{2+} (mg/L)	0.06	0.08	**0.92**	0.15	0.19
Na^{+} (mg/L)	**0.92**	0.27	−0.14	0.09	−0.12
HCO_3^{-} (mg/L)	−0.40	−0.09	0.26	0.02	**0.86**
Cl^{-} (mg/L)	**0.97**	−0.02	0.10	0.04	−0.17
SO_4^{2-} (mg/L)	0.12	**0.94**	−0.14	0.18	−0.01
SiO_2 (mg/L)	0.15	0.03	0.13	**0.97**	0.01
% of variance	42.71	18.26	12.81	10.59	9.40
Cumulative %	42.71	60.96	73.78	84.37	93.77

Bold values = loadings > 0.50.

Table 5. *Chemical constituents (meq/L) of seawater and freshwater and the calculated fraction of seawater from the monitored wells.*

Chemical Constituents	Seawater[a]	Collected Samples, March 2012	Freshwater[a]	Change, March 2012
Ca^{2+}	21.05	19.00	3.04	14.52
Mg^{2+}	32.30	4.49	0.99	1.00
Na^{+}	1126.00	29.90	0.04	−59.88
K^{+}	10.96	4.49	0.12	3.51
HCO_3^{-}	1.49	2.6	5.83	−2.88
Cl^{-}	461.11	41.23	4.82	0.00
SO_4^{2-}	45.80	9.34	0.83	4.93
f_{sea}	100.00	7.97	–	

[a] After Mondal *et al.* (2011).

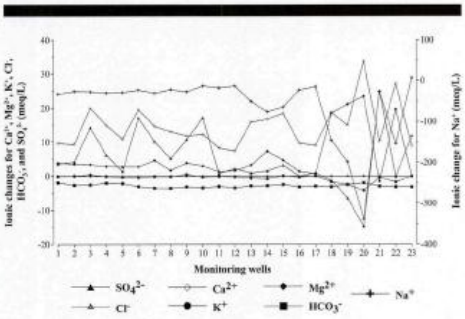

Figure 4. Ionic changes in the groundwater samples of the coastal aquifers (Saudi Gulf of Aqaba).

ions. When the seawater, which is dominated by Na^{+} and Cl^{-} ions, intrudes the coastal aquifers, an exchange of cations occurs (Appelo and Postma, 2005). This is clearly indicated by a relationship between Na^{+} and Ca^{2+} and a negative value ΔC_{Na} in samples. Such a process is highly influenced by seawater signature, *i.e.* when more seawater intrudes the aquifer, a negative value of ionic ΔC_{Na} increases (see Figure 5a). This influence is comparatively

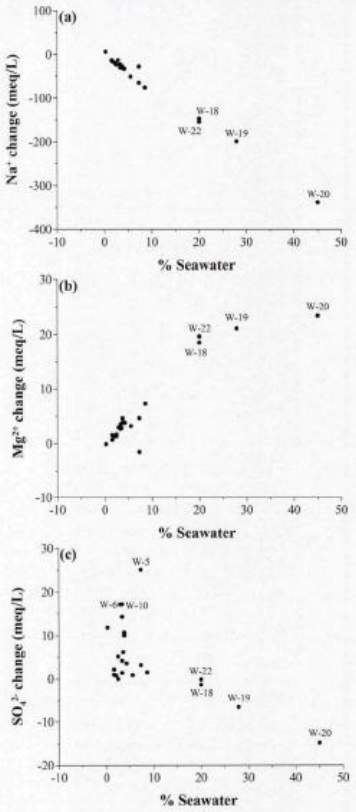

Figure 5. Ionic changes (ΔC) for (a) Na^{+}, (b) Mg^{2+}, and (c) SO_4^{2-} in the collected samples.

higher in the wells (W-18, W-19, W-20, and W-22) where negative Na^{+}-ionic exchanges of less than −100 meq/L are observed. The element of Mg^{2+} showed a positive ΔC_{Mg} (>20 meq/L) in the samples that are marked by higher seawater signature (see Figure 5b). The downward trend for Na^{+} and upward trend for Mg^{2+} with the increased fraction of seawater show the effects of seawater intrusion on the studied groundwater. This phenomenon can be observed by a negative value of ΔC_{Na} for Na^{+} and a positive value of ΔC_{Mg} for Mg^{2+}. In the case of ionic exchanges for SO_4^{2-} (Figure 5c), it was >15.0 meq/L for groundwater samples (W-6, W-10, and W-5) collected from around the outcropping gypsum area, whereas the calculated seawater fractions of groundwaters of W-18, W-19, W-20, and W-22 monitoring wells were >20%. The ΔC_{SO_4} in both cases were within approximately 90° phase.

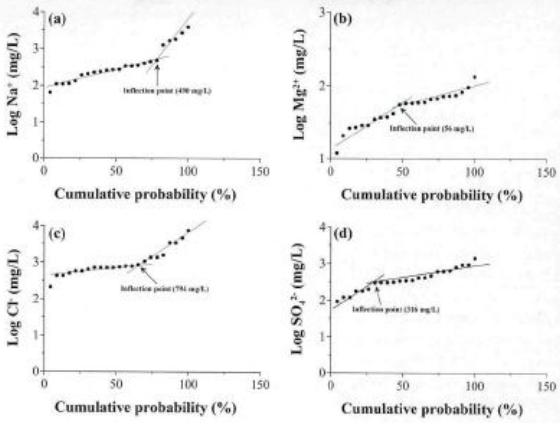

Figure 6. Cumulative probability curves for the distribution of (a) Na^+, (b) Mg^{2+}, (c) Cl^-, and (d) SO_4^{2-} in the studied groundwater.

Intersection of Seawater Mixing

Results of the interpretation of cumulative probability curves for Na^+, Mg^{2+}, Cl^-, and SO_4^{2-} are shown in Figure 6. The intersection points on the plot (Figure 6) can be considered as regional threshold values (T) in differentiating the effects of seawater mixing in the samples of the study area. The calculated (T) values are 490 mg/L, 56 mg/L, 794 mg/L, and 316 mg/L for Na^+, Mg^{2+}, Cl^-, and SO_4^{2-}, respectively. These values were then used to calculate SMI values (from Equation [4]), which varied from 0.395 to 7.922. Figure 7 shows the plots of SMI with EC and Cl^-, which indicate 13 of 23 groundwater samples as saline (with EC > 3000 µS/cm), representing about 57% of the studied samples. The SMI values for these samples range between 0.825 and 7.922. As shown in the plot, one sample (*i.e.* W-23) is fresh with SMI < 0.5, EC < 1500 µS/cm, and Cl^- < 215 mg/L. The SMI values for the groundwater samples influenced by seawater intrusion are >5.0.

CONCLUSIONS

This study provides an outline for geochemical processes controlling the chemistry of the groundwater aquifer under the Saudi Gulf of Aqaba coast. Groundwater in the study area is dominantly characterized by Ca^{2+}–Cl^-–SO_4^{2-} and Na^+–Cl^-–SO_4^{2-} as hydrochemical facies. Major ionic compositions (including the higher concentration of Cl^- and TDS) clearly indicate the effects of seawater intrusion, and the resultant salinization of the studied groundwater.

Besides the major chemical compositions, ionic ratios are efficiently used to delineate seawater intrusion. Among others, the ratios of HCO_3^-/Cl^-, Na^+/Ca^{2+}, Ca^{2+}/Cl^-, Mg^{2+}/Cl^-, and Ca^{2+}/SO_4^{2-} appeared the most useful indicators. The processes that govern changes in the groundwater composition of the study area (as revealed by statistical analysis) are mainly linked with five factors. The first factor is associated with the processes of mineral dissolution involving water and the geological media. The second factor is associated with human activities, weathering processes, and marine inputs. The third one is linked to evaporation/salinization of the groundwater. The fourth one is attributed to long water residence time, in which the relatively elevated Cl^-, Ca^{2+}, and SO_4^{2-} concentrations indicate a slow path flow within the salt-enriched media (probably marine sediments). The fifth factor is associated with evaporation/salinization of groundwater and dissolution of sediments.

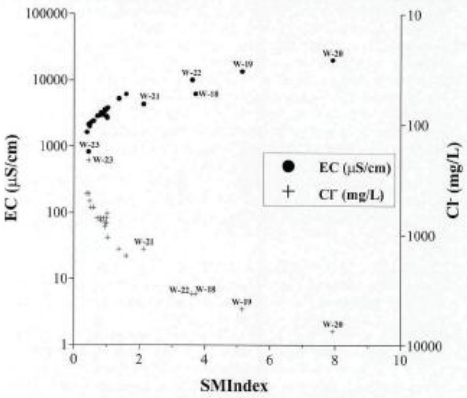

Figure 7. Cross-plot of seawater mixing index vs. electrical conductivity and Cl^- of the studied groundwater samples.

The mixing rate of seawater intrusion during the sampling period is about 7.97%. The most dominant process that takes place with the freshwater–seawater mixing is the cation exchange, which occurs mainly as a direct exchange between Na^{+} with Ca^{2+} and Mg^{2+}. In the case of SO_4^{2-}, the ionic exchanges of >15.0 meq/L are observed in the groundwater samples collected from gypsum outcrop area. Variations in the SMI values (0.395 to 7.922) and the TDS values (406 to 10,018 mg/L) indicate that 57% of the sampled water is saline with EC > 3000 μS/cm and SMI values >0.8.

ACKNOWLEDGMENTS

This work is financially supported by the National Plan for Science, Technology and Innovation program, King Saud University, Saudi Arabia (Project No. 11-WAT1731-02). We thank the staff at General Directorate of Water in Al-Bad' City (Ministry of Water & Electricity, Saudi Arabia) for their help and valuable information during the course of the field work. The two anonymous reviewers and the editorial board of *Journal of Coastal Research* suggested their constructive comments to improve the article. We are thankful to them.

LITERATURE CITED

Al-Agha, M. and El-Nakhal, H., 2004. Hydrochemical facies of groundwater in the Gaza Strip, Palestine. *Hydrological Sciences Journal*, 49(3), 359–371.

Al-Ahmadi, M.E., 2009. Hydrogeology of the Saq Aquifer Northwest of Tabuk, Northern Saudi Arabia. *Journal of King Abdulaziz University-Earth Sciences*, 20(1), 51–66.

APHA (American Public Health Association), 1998. *Standard Methods for the Examination of Water and Wastewater*, 20th edition Washington, DC, 46p.

Appelo, C.A.J. and Postma, D., 2005. *Geochemistry, Groundwater and Pollution*, 2nd edition. Rotterdam: Balkema, 668p.

Assaf, G. and Kessler, J., 1976. Climate and energy in the Gulf of Aqaba (Elat). *Monthly Weather Review*, 104(4), 381–385.

Barbecot, F.; Marlin, C.; Gibert, E., and Dever, L., 2000. Hydrochemical and isotopic characterisation of the Bathonian and Bajocian coastal aquifer of the Caen area (Northern France). *Applied Geochemistry*, 15(6), 791–805.

Barker, A.; Newton, R., and Bottrell, S., 1998. Processes affecting groundwater chemistry in a zone of saline intrusion into an urban aquifer. *Applied Geochemistry*, 13(6), 735–749.

Batayneh, A.T., 2006. Use of electrical resistivity methods for detecting subsurface fresh and saline water and delineating their interfacial configuration: a case study of the eastern Dead Sea coastal aquifers, Jordan. *Hydrogeology Journal*, 14(7), 1277–1283.

Batayneh, A.; Elawadi, E., and Al-Arifi, N., 2010. Use of geoelectrical technique for detecting subsurface fresh and saline water: a case study of the eastern Gulf of Aqaba coastal aquifer, Jordan. *Journal of Coastal Research*, 26(6), 1079–1084.

Batayneh, A.; Elawadi, E.; Mogren, S.; Ibrahim, E., and Qaisy, S., 2012a. Groundwater quality of the shallow alluvial aquifer of Wadi Jazan (Southwest Saudi Arabia) and its suitability for domestic and irrigation purpose. *Scientific Research and Essays*, 7(3), 352–364.

Batayneh, A.; Ghrefat, H., and Diabat, A., 2012b. Lineament characterization and their tectonic significance using gravity data and field studies in the Al-Jufr area, southeastern Jordan Plateau. *Journal of Earth Science*, 23(6), 873–880.

Batayneh, A. and Zumlot, T., 2012. Multivariate statistical approach to geochemical methods in water quality factor identification; application to the shallow aquifer system of the Yarmouk Basin of north Jordan. *Research Journal of Environmental and Earth Sciences*, 4(7), 756–768.

Briz-kishore, B. and Murali, G., 1992. Factor analysis for revealing hydrogeochemical characteristics of a watershed. *Environmental Geology*, 19(1), 3–9.

Clark, M., 1986. Explanatory notes to the geologic map of the Al Bad' Quadrangle, sheet 28A, Kingdom of Saudi Arabia. Saudi Arabian Deputy Ministry for Mineral Resources. *Geoscience Map Series GM-81A, C*, scale 1:250,000, with text, 46p.

Cloutier, V.; Lefebvre, R.; Therrien, R., and Savard, M., 2008. Multivariate statistical analysis of geochemical data as indicative of the hydrogeochemical evolution of groundwater in a sedimentary rock aquifer system. *Journal of Hydrology*, 353(3–4), 294–313.

Diamantis, I.B. and Petalas, C.P., 1989. Seawater intrusion into coastal aquifers of Thrace and its impact on the environment. *Toxicological & Environmental Chemistry*, 20–21(1), 291–305.

Domenico, P.A. and Schwartz, F.W., 1990. *Physical and Chemical Hydrogeology*. New York: Wiley, 824p.

Edet, A. and Okereke, C., 2002. Delineation of shallow groundwater aquifers in the coastal plain sands of Calabar area (Southern Nigeria) using surface resistivity and hydro geological data. *Journal of African Earth Sciences*, 35(3), 433–443.

Elawadi, E.; Zaman, H.; Batayneh, A.; Mogren, S.; Laboun, A.; Ghrefat, H., and Zumlot, T., 2013. Structural interpretation of the Ifal Basin, northwestern Saudi Arabia, from aeromagnetic data: hydrogeological and environmental implications. *Exploration Geophysics*. In press.

El Moujabber, E.; Bou Samra, M.; Darwish, B., and Atallah, T., 2006. Comparison of different indicators for groundwater contamination by seawater intrusion on the Lebanese Coast. *Water Resources Management*, 20(2), 161–180.

Fahmy, M., 2003. Water quality in the Red Sea coastal waters (Egypt): analysis of spatial and temporal variability. *Chemistry and Ecology*, 19(1), 67–77.

Farnham, I.; Johannesson, K.; Singh, A.; Hodge, V., and Stetzenbach, K., 2003. Factor analytical approaches for evaluating groundwater trace element chemistry data. *Analytica Chimica Acta*, 490(1–2), 123–138.

Farnham, I.; Stetzenbach, K.; Singh, A., and Johannesson, K., 2000. Deciphering groundwater flow systems in Oasis Valley, Nevada, using trace element chemistry, multivariate statistics, and geographical information system. *Mathematical Geology*, 32(8), 943–968.

Farooq, M.; Abdul Malik, M.; Hussain, A., and Abbasi, H., 2010. Multivariate statistical approach for the assessment of salinity in the periphery of Karachi, Pakistan. *World Applied Science Journal*, 11(4), 379–387.

Hall, J., 1975. Bathymetric chart of the Straits of Tiran. *Israel Journal of Earth Sciences*, 24(3–4), 69–72.

Howard, K.W.F. and Lloyd, J.W., 1983. Major ion characterization of coastal saline ground waters. *Groundwater*, 21(4), 429–437.

Kim, J.; Kim, R., and Chang, H., 2003. Hydrogeochemical characterization of major factors affecting the quality of shallow groundwater in the coastal area at Kimje in South Korea. *Environmental Geology*, 44(4), 478–489.

Kim, K.Y.; Park, Y.S.; Kim, G.P., and Park, K.H., 2009. Dynamic freshwater–saline water interaction in the coastal zone of Jeju Island, South Korea. *Hydrogeology Journal*, 17(3), 617–629.

Lee, J.Y. and Song, S.H., 2007a. Evaluation of groundwater quality in coastal areas: Implications for sustainable agriculture. Environmental Geology, 52(7), 1231–1242.

Lee, J.Y. and Song, S.H., 2007b. Groundwater chemistry and ionic ratios in a western coastal aquifer of Buan, Korea: implication for seawater intrusion. *Geosciences Journal*, 11(3), 259–270.

Liu, C.; Lin, K., and Kuo, Y., 2003. Application of factor analysis in the assessment of groundwater quality in a blackfoot disease area in Taiwan. *Science of the Total Environment*, 313(1–3), 77–89.

Love, D.; Hallbauer, D.; Amos, A., and Hranova, R., 2004. Factor analysis as a tool in groundwater quality management: two southern African case studies. *Physics and Chemistry of the Earth*, 29(15–18), 1135–1143.

Maillard, C. and Soliman, G., 1986. Hydrography of the Red Sea and exchange with Indian Ocean in summer. *Oceanologica Acta*, 9(3), 249–269.

Melloul, A. and Collin, M., 2006. Hydrogeological changes in coastal aquifers due to sea level rise. *Ocean Coast Management*, 49(5–6), 281–297.

Mondal, N.C.; Singh, V.P.; Singh, S., and Singh, V.S., 2011. Hydrochemical characteristic of coastal aquifer from Tuticorin, Tamil

Nadu, India. *Environmental Monitoring and Assessment*, 175(1), 531–550.
Mondal, N.C.; Singh, V.P.; Singh, V.S., and Saxena, V.K., 2010. Determining the interaction between groundwater and saline water through groundwater major ion chemistry. *Journal of Hydrology*, 388(1–2), 100–111.
Mondal, N.C.; Singh, V.S.; Saxena, V.K., and Prasad, R.K., 2008. Improvement of groundwater quality due to fresh water ingress in Potharlanka Island, Krishna delta, India. *Environmental Geology*, 55(3), 595–603.
Morcos, S.A., 1970. Physical and chemical oceanography of the Red Sea. *Oceanography and Marine Biology: An Annual Review*, 8, 73–202.
Nwankwoala, H. and Udom, G., 2011. Hydrochemical facies and ionic ratios of groundwater in Port Harcourt, Southern Nigeria. *Research Journal of Chemical Sciences*, 1(3), 87–101.
Piper, A., 1944. A graphic procedure in the geochemical interpretation of water-analysis. *Transactions—American Geophysical Union*, 25(6), 914–928.
Razack, M. and Dazy, J., 1990. Hydrogeochemical characterization of groundwater mixing in sedimentary and metamorphic reservoirs with combined use of Pipers principle and factor analysis. *Journal of Hydrology*, 114(3–4), 371–393.
Sanchez-Martos, F.; Pulido-Bosch, A.; Molina-Sanchez, L., and Vallejos Izquierdo, A., 2002. Identification of the origin of salinization in groundwater using minor ions (Lower ANDARAX, Southeast. Spain). *Science of the Total Environment*, 29(1–3), 43–58.
Sarma, V.V.J. and Krishnaiah, N., 1976. Quality of groundwater in the coastal aquifer near Visakhapatnam, India. *Ground Water*, 14(5), 290–295.
Sharma, P.V., 1997. *Environmental and Engineering Geophysics*. Cambridge, U.K.: Cambridge University Press, 475p.
Sharma, S., 1996. Applied Multivariate Techniques. New York: Wiley, 493p.
Silva-Filho, E.V.; Sobral Barcellos, R.; Emblanch, C.; Blavoux, B.; Maria Sella, S.; Daniel, M.; Simler, R., and Cesar Wasserman, J., 2009. Groundwater chemical characterization of a Rio de Janeiro coastal aquifer, SE-Brazil. *Journal of South American Earth Sciences*, 27(1), 100–108.
Stetzenbach, K.; Hodge, V.; Guo, C.; Farnham, I., and Johannesson, K., 2001. Geochemical and statistical evidence of deep carbonate groundwater within overlying volcanic rock aquifers/aquitards of southern Neveda, USA. *Journal of Hydrology*, 243(3–4), 254–271.
Subyani, A. and Al-Ahmadi, M., 2010. Multivariate statistical analysis of groundwater quality in Wadi Ranyah, Saudi Arabia. *Journal of King Abdulaziz University-Earth Sciences*, 21(2), 29–46.
Tellam, J.H. and Lloyd, J.W., 1986. Problems in the recognition of seawater intrusion by chemical means: an example of apparent chemical equivalence. *Quarterly Journal of Engineering Geology and Hydrogeology*, 19(4), 389–398.
WHO (World Health Organization), 1984. *Guideline of drinking quality*. Washington, DC: WHO, 355p.
WHO, 2008. *Guidelines for Drinking-Water Quality, 3rd edition*. Geneva, Switzerland: WHO, 494p.
Wyn Hughes, G. and Johnson, R., 2005. Lithostratigraphy of the Red Sea region. *GeoArabia*, 10(3), 49–126.
Wyn Hughes, G.; Perincek, D.; Grainger, D.J.; Abu-Behait, A., and Jarad, A., 1999. Lithostratigraphy and depositional history of part of the Midyan region, northwestern Saudi Arabia. *GeoArabia*, 1(4), 503–542.